

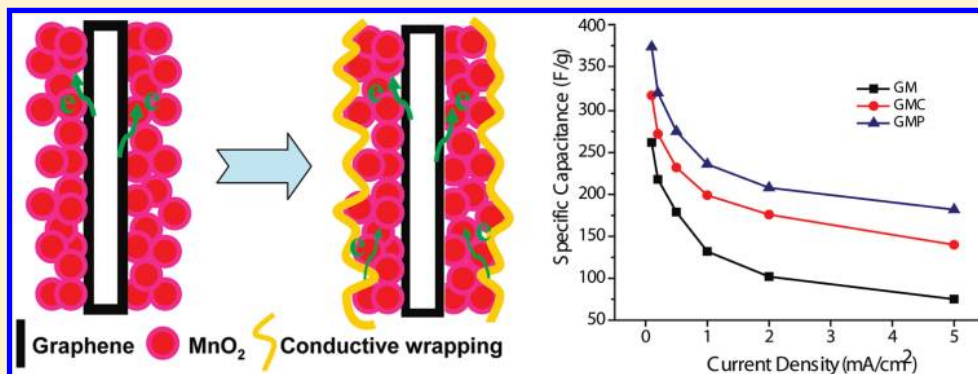
# Enhancing the Supercapacitor Performance of Graphene/MnO<sub>2</sub> Nanostructured Electrodes by Conductive Wrapping

Guihua Yu,<sup>†</sup> Liangbing Hu,<sup>‡</sup> Nian Liu,<sup>§</sup> Huiliang Wang,<sup>‡</sup> Michael Vosgueritchian,<sup>†</sup> Yuan Yang,<sup>‡</sup> Yi Cui,<sup>\*,†</sup> and Zhenan Bao<sup>\*,†</sup>

<sup>†</sup>Department of Chemical Engineering, <sup>‡</sup>Department of Materials Science and Engineering, and <sup>§</sup>Department of Chemistry, Stanford University, Stanford, California 94305, United States.

**S** Supporting Information

## ABSTRACT:



MnO<sub>2</sub> is considered one of the most promising pseudocapactive materials for high-performance supercapacitors given its high theoretical specific capacitance, low-cost, environmental benignity, and natural abundance. However, MnO<sub>2</sub> electrodes often suffer from poor electronic and ionic conductivities, resulting in their limited performance in power density and cycling. Here we developed a “conductive wrapping” method to greatly improve the supercapacitor performance of graphene/MnO<sub>2</sub>-based nanostructured electrodes. By three-dimensional (3D) conductive wrapping of graphene/MnO<sub>2</sub> nanostructures with carbon nanotubes or conducting polymer, specific capacitance of the electrodes (considering total mass of active materials) has substantially increased by ~20% and ~45%, respectively, with values as high as ~380 F/g achieved. Moreover, these ternary composite electrodes have also exhibited excellent cycling performance with >95% capacitance retention over 3000 cycles. This 3D conductive wrapping approach represents an exciting direction for enhancing the device performance of metal oxide-based electrochemical supercapacitors and can be generalized for designing next-generation high-performance energy storage devices.

**KEYWORDS:** Supercapacitor electrodes, conductive polymer, MnO<sub>2</sub>, carbon nanotubes, graphene

Supercapacitors, also known as electrochemical capacitors, represent a unique class of energy storage devices that exhibit high power capability, long cycle lifetime, and fast charge and discharge rates, with a range of applications from portable electronics, and memory backup systems, to hybrid electric vehicles, and industrial scale power and energy management.<sup>1–4</sup> However, the energy storage density of existing supercapacitors is limited, generally an order of magnitude lower than that of batteries.<sup>5</sup> Currently, improving the energy density while maintaining the high power density and cycling stability for supercapacitor devices remains a primary research focus in the field. Pseudocapacitive transition-metal oxides such as RuO<sub>2</sub>, NiO, and MnO<sub>2</sub>,<sup>6–8</sup> have been studied extensively as active electrode materials for supercapacitors owing to their high energy density and large charge-transfer-reaction pseudocapacitance which is based on fast and reversible redox reactions at the electrode surface, resulting in much higher specific capacitance exceeding that of carbon-based materials

using electric double layer charge storage. Although MnO<sub>2</sub> is considered to be the most attractive oxide material owing to high abundance of Mn, low cost, and environmental friendliness, the poor conductivity of MnO<sub>2</sub> (10<sup>–5</sup>–10<sup>–6</sup> S/cm) remains a major challenge and limits the rate capabilities for high power performance, thus hindering its wide applications in energy storage systems.<sup>9</sup>

To improve the electrical conductivity of MnO<sub>2</sub>-based electrodes for optimized electrochemical performance, considerable research efforts have been placed on exploring hybrid composite structures where MnO<sub>2</sub> is combined with highly conductive materials such as metal nanostructures,<sup>10</sup> carbon nanotubes (CNTs),<sup>11–14</sup> graphene,<sup>15,16</sup> or conducting polymers (CPs),<sup>17,18</sup> for improved electrochemical performance. Among various nanocomposite

**Received:** August 2, 2011

**Revised:** September 12, 2011

**Published:** September 26, 2011

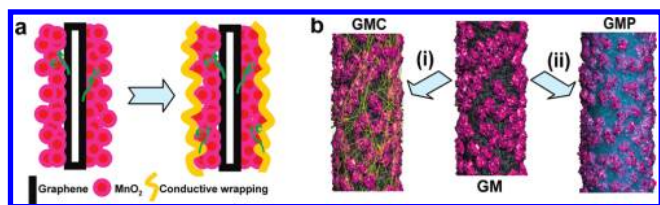


**Figure 1.** (a) Schematic illustration showing conductive wrapping of graphene/MnO<sub>2</sub> (GM) to introduce an additional electron transport path (in a discharge cycle). (b) Schematic of graphene/MnO<sub>2</sub>/CNT (GMC) and graphene/MnO<sub>2</sub>/conducting polymer (GMP) systems formed by wrapping of GM nanostructures with CNTs or conducting polymers (black, graphene; rose, MnO<sub>2</sub>; yellow, CNTs; blue, conducting polymer).

materials developed so far, hybrid graphene/MnO<sub>2</sub> (GM) nanostructures based supercapacitor electrodes prepared with low-cost materials and scalable processes hold particular promise for potentially large-scale energy storage systems. To realize many practical applications that require large capacitance and high energy storage, the high mass loading of active MnO<sub>2</sub> materials usually leads to the increased electrode resistance and the decreased specific capacitance, because MnO<sub>2</sub> becomes densely packed with limited electrochemically active surface area, resulting in only a very thin top layer (up to a few hundreds of nanometers) of oxide nanomaterials participating in the charge storage process.<sup>9</sup>

To solve these critical problems, we developed a “three-dimensional (3D) conductive wrapping” method to rationally design ternary systems based on graphene/MnO<sub>2</sub>/CNT (GMC) and graphene/MnO<sub>2</sub>/poly(3,4-ethylenedioxythiophene)–poly(styrenesulfonate) (PEDOT:PSS) (GMP) composites for high-performance electrochemical electrodes. The novel composite electrodes exhibited much enhanced capacitance performance and rate capability, and excellent cycling stability compared to those of GM nanostructured electrodes (Figure 1). An ultrathin layer of single-walled CNTs (SWNTs) or conducting polymer that wraps around graphene/MnO<sub>2</sub> three-dimensionally not only provides an additional electron transport path besides the graphene layer underneath MnO<sub>2</sub> nanomaterials but actively participates in the charge storage process as both can contribute to the energy storage of the whole film via electric double layer capacitance or pseudocapacitance. Such 3D conductive wrapping approach would provide a promising design direction for optimizing the electrochemical performance of insulating metal-oxide based electrode materials and could be generally applicable to many promising but challenging energy storage electrode materials in which the electron transport limits the device performance.

To demonstrate this idea, we chose GM nanostructured textile electrodes in our studies as a platform to investigate the effect of conducting wrapping on improving the electrochemical performance of a GM-based system. The GM–textile electrodes were prepared by a two-step solution-based coating process developed recently,<sup>16</sup> and the conductive wrapping with CNTs to form a GMC system was achieved by simply dipping GM–textiles into a 0.2 mg/mL SWNT ink solution and subsequently drying in a vacuum oven at 100 °C for 10 min (see Supporting Information for experimental details). Figure 2a shows a representative scanning electron microscope (SEM) image of GMC nanostructures, demonstrating that an ultrathin film of interconnected SWNT network (only ~0.1 mg/cm<sup>2</sup> loading) was uniformly coated on the nanoflower-shaped MnO<sub>2</sub> surface, effectively wiring up the MnO<sub>2</sub> nanoparticles while leaving their largest possible electroactive surface area for charge storage.

To evaluate the electrochemical performance of these hybrid nanostructured textiles as active supercapacitor electrodes, we performed electrochemical impedance spectroscopy (EIS), cyclic voltammetry (CV), and galvanostatic charge–discharge measurements in a three-electrode configuration. The impedance curve for GMC-based textile electrodes measured in a 0.5 M Na<sub>2</sub>SO<sub>4</sub> electrolyte solution (Figure 3a) shows that the equivalent series resistances (ESR) extracted from high frequency (100 kHz) was estimated to be ~41 Ω, in contrast to ~87 Ω for GM-based electrodes, which reflects the higher conductivity achieved in the GMC system. The more vertical shape at lower frequencies for GMC indicates a more capacitive behavior of electrodes. CVs for GMC–textile electrodes (Figure 2b) in the potential window of 0–0.85 V at various scan rates (5–100 mV/s) show more rectangular shape for all scan rates than those of GM-based electrodes, indicating that GMC electrodes exhibited lower resistance and more ideal supercapacitor behavior.<sup>2</sup> At the same scan rate of 100 mV/s, Figure 3b shows that the resulting current from GMC is also higher than that of GM–textile, suggesting that conductive CNT wrapping facilitates the electron transport in the film and enhances the electrochemical utilization of MnO<sub>2</sub>. The improved electrochemical performance was also confirmed by galvanostatic charge–discharge tests performed under different current densities. Figure 2c shows the galvanostatic charge–discharge curves for the GMC system at three different current densities of 2, 1, and 0.5 mA/cm<sup>2</sup>, respectively. Figure 3c shows that at the same current density of 0.5 mA/cm<sup>2</sup>, the charge–discharge time for GMC system was substantially prolonged (~80% increase) over the GM system, and moreover, the linear voltage–time profile and the highly symmetric charge/discharge characteristics were indicative of good capacitive behavior achieved by the GMC system. Figure 3d summarizes the specific capacitance at different current densities calculated from the charge–discharge curves (considering total mass of active electrode materials including CNTs) and demonstrates that the hybrid GMC-based textiles yielded the enhanced capacitance performance with ~20–25% increase in specific capacitance compared to that of GM-based textiles. Meanwhile, GMC-based electrodes exhibited better rate capability, with only ~35% capacitance loss when current density increases by a factor of 10 (from 0.5 to 5 mA/cm<sup>2</sup>) compared to ~60% loss for GM-based electrodes. The enhanced capacitance and rate capability can be attributed to shorter ion diffusion path and increased electronic conductivity.

In addition to the GMC system achieved by conductive wrapping with CNTs, conducting polymers such as PEDOT:PSS could be quite useful for further enhancement of the composite electrodes’ electrochemical performance. Similarly, GMP-based electrodes were prepared by coating GM–textiles with commercially available PEDOT:PSS solution (Clevios PH1000, 1:10 diluted in deionized water) via the “dip and dry” process (see experimental details in the Supporting Information). A typical high-magnification SEM image (Figure 2d) of GMP nanostructures shows that a very thin but continuous layer of conducting polymer film (~0.2 mg/cm<sup>2</sup> deposited) was well distributed on GM nanostructures, and PEDOT:PSS polymer was intertwined and intimately bound with the flower-like MnO<sub>2</sub> nanoparticles, serving dual functions as both conductive additives and binder materials.<sup>12,19</sup> The PEDOT:PSS polymer can potentially offer better interconnectivity within MnO<sub>2</sub> nanoparticles and meanwhile can participate in the charge storage process through the redox-reaction-based pseudocapacitance.

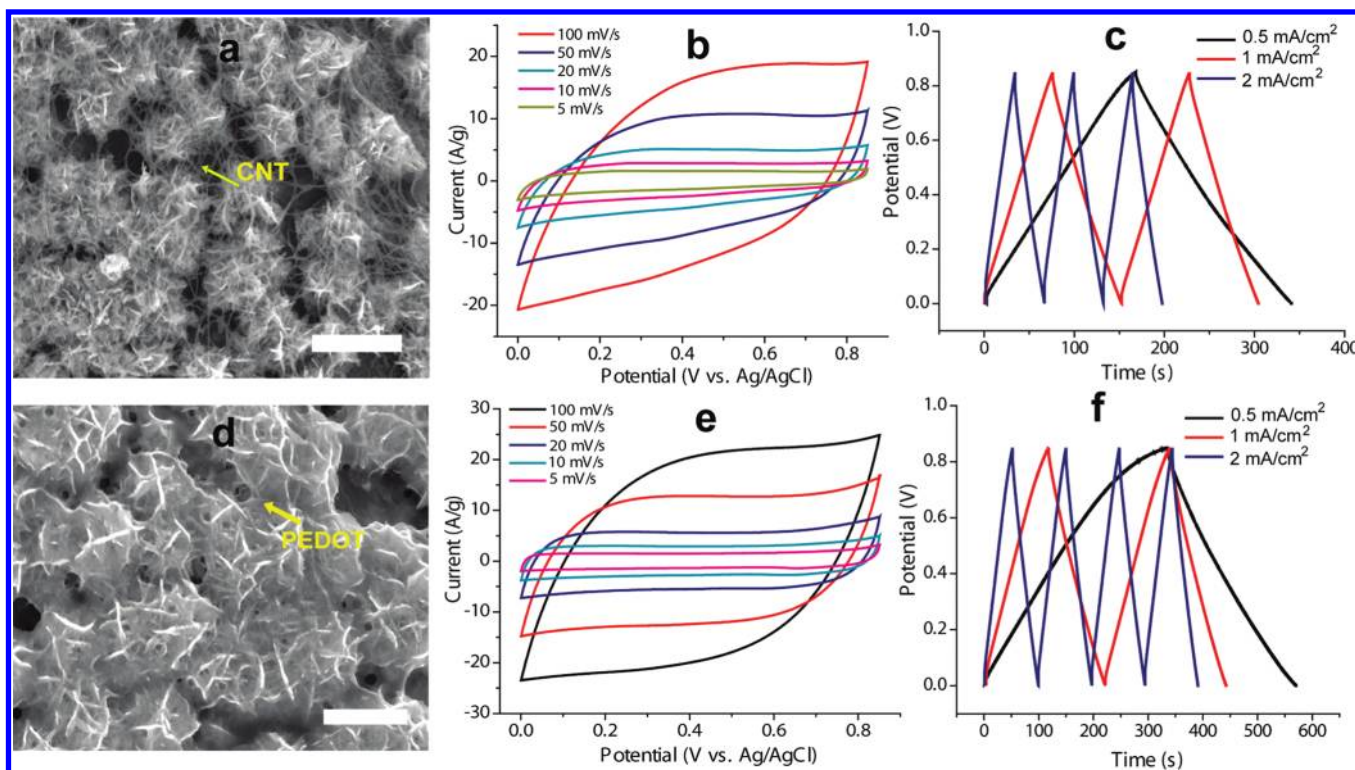


**Figure 2.** Conductive wrapping of GM nanostructured electrodes with CNTs and conducting polymer PEDOT:PSS. (a) Representative SEM image showing SWNTs interconnected with graphene/MnO<sub>2</sub> forming GMC nanostructures. Scale bar: 1  $\mu\text{m}$ . (b) CV curves for GMC—textile electrodes at different scan rates (5–100 mV/s) in 0.5 M aqueous Na<sub>2</sub>SO<sub>4</sub> electrolyte. (c) Galvanostatic charge—discharge measurement of GMC-based electrodes at different current densities of 2, 1, and 0.5 mA/cm<sup>2</sup>. (d) Typical SEM image showing graphene/MnO<sub>2</sub>/PEDOT:PSS nanostructures (GMP). Scale bar: 1  $\mu\text{m}$ . (e) CV curves for GMP—textile electrodes at various scan rates (5–100 mV/s). (f) Galvanostatic charge—discharge curves of GMP-based electrodes at various current densities.

The GMP-based electrode system demonstrates excellent electrochemical properties with substantially enhanced capacitance performance and even better rate capability when compared with the GMC-based system. First, the Nyquist plots of three different supercapacitor electrodes (Figure 3a) show the most vertical line in a low-frequency region and the lowest ESR value ( $\sim 27 \Omega$ ) for GMP system proving that GMP-based electrodes behave as the nearly ideal capacitors. Rate-dependent CVs for GMP-based electrodes (Figure 2e) clearly show almost rectangular-shaped curves for all scan rates from 5 to 100 mV/s, confirming the highest conductivity of electrodes and the best capacitive behavior among all three systems. Under the scan rate of 100 mV/s, GMP electrodes yielded the largest current and resulted in much higher capacitance (Figure 3b), which is believed to be due to the synergistic effects from each component of composite electrodes: conducting graphene backbone on textile fibers, mesoporous flower-like MnO<sub>2</sub> nanoparticles, and conductive wrapping layer of PEDOT:PSS that further boosts the electrical conductivity and contributes the redox-based pseudocapacitance. Galvanostatic charge—discharge measurements were further taken at various current densities, as shown in Figure 2f. At the same current density of 0.5 mA/cm<sup>2</sup> (Figure 3c), the charge storage capacity for the GMP system was significantly improved, with  $\sim 40\%$  increase in discharge time over GMC system and  $\sim 160\%$  increase over GM system. More importantly, the summary plot of specific capacitance versus current density (Figure 3d) demonstrates that the hybrid GMP-based textile electrodes exhibited significantly enhanced capacitance performance with specific

capacitance as high as  $\sim 380 \text{ F/g}$  achieved (based on total mass of active electrode materials including PEDOT:PSS) at a current density of 0.1 mA/cm<sup>2</sup>,  $\sim 45\%$  increase compared with that of a GM-based electrode system. Moreover, the rate performance of GMP system was also improved with  $>70\%$  capacitance maintained as current density increases from 0.5 to 5 mA/cm<sup>2</sup>, which is better than that of both GMC and GM systems. Although GMP system offers higher specific capacitance due to large pseudocapacitance contributed from conductive polymer, the wrapping with CNTs can be advantageous in those applications that require high operation voltages owing to their better electrochemical stability across a large voltage range and environmental safety.<sup>20</sup>

Cycling performance is another key factor in determining the supercapacitor electrodes for many practical applications. Excellent cycling stability is crucial for real supercapacitor operations. The cycling tests for all three different electrode systems were carried out using the same current density of 1 mA/cm<sup>2</sup>. Figure 4a compares the cycling stability of three systems and shows that  $\sim 93\%$ ,  $\sim 96\%$ , and  $\sim 95\%$  capacitance was retained over 3000 cycles of charging and discharging for GM-, GMC-, and GMP-based electrodes, respectively. All three electrode systems demonstrate much better cycling performance compared to those reported in previous work (typically 75–85% retention over 1000 cycles),<sup>13,21,22</sup> thanks to hierarchical structures of graphene/MnO<sub>2</sub>—textiles.<sup>16</sup> The slightly better cycling stability of GMC and GMP systems over the GM system suggests that 3D conductive wrapping could possibly help stabilize the MnO<sub>2</sub> nanomaterials mechanically and keep them bound together during the cycling tests to avoid MnO<sub>2</sub> material

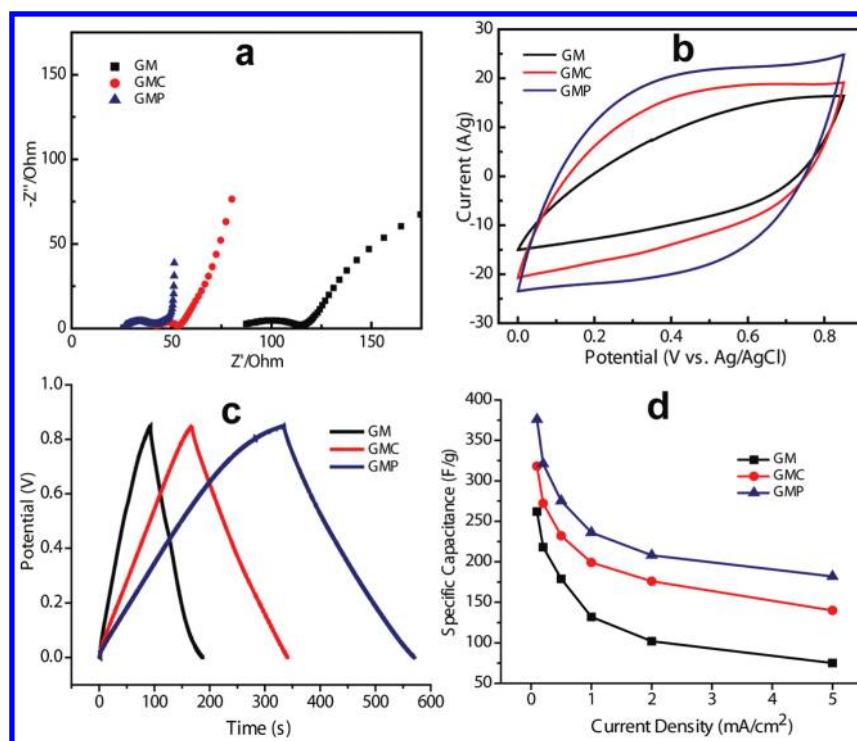


**Figure 3.** Comparison of electrochemical performance of GM, GMC, and GMP-based nanostructured electrodes. (a) Impedance comparison curves for GM- (black curve), GMC- (red curve), and GMP-based (blue curve) textile electrodes.  $Z'$  is real impedance and  $Z''$  is imaginary impedance. (b) Comparison of CVs for GM- (black), GMC- (red), and GMP-based (blue) electrodes at the same scan rate of 100 mV/s. (c) Galvanostatic charge–discharge curves for GM, GMC, and GMP composite electrodes at current density of 0.5 mA/cm<sup>2</sup>. (d) Summary plot of specific capacitance values for three different electrode systems: GM-, GMC-, and GMP-based textiles at various current densities.

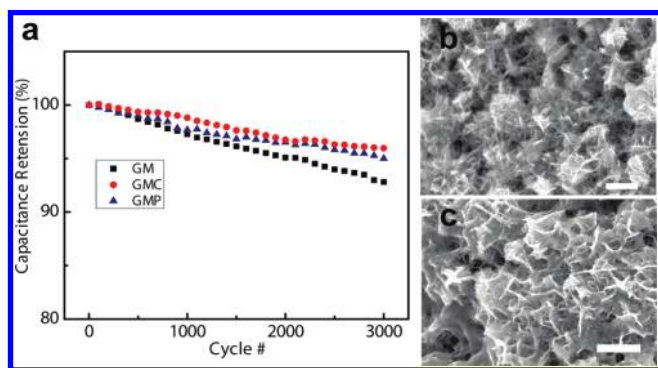


**Figure 4.** Cycling performance of hybrid nanostructured electrodes. (a) Comparison of cycling performance for three hybrid systems showing capacitance retention of ~93%, ~96%, and ~95% after 3000 cycles of charging and discharging at current density of 1 mA/cm<sup>2</sup> for GM, GMC, and GMP, respectively. (b, c) SEM images of GMC- and GMP-based textiles after 3000 cycles showing that the MnO<sub>2</sub> nanoflowers were still wrapped with conductive layers and the whole structural integrity of active electrode materials was well maintained. Scale bars: 1 μm.

loss and film detachment from electrode surfaces due to Mn dissolution into electrolyte solutions, which are common causes for limited cycling life of MnO<sub>2</sub>-based electrodes.<sup>23</sup> Compared to conventional preparation methods for metal oxide based composite electrodes that physically mix active materials with insulating binder materials such as poly(tetrafluoroethylene) (PTFE) or poly(vinylidene fluoride) (PVDF), and conductive additives such as carbon black,<sup>7,8,11,12</sup> the 3D conductive

wrapping approach could serve dual functions of improving the electrical conductivity and the stability of electrodes, therefore greatly enhancing the electrochemical performance and cycling performance. In fact, we characterized the morphology and structure of our hybrid electrodes after 3000 cycles and found that the nanoflower MnO<sub>2</sub> structures were still well-maintained and the whole structural integrity of active electrode materials remained, as shown in panels b and c of Figure 4.

In summary, by 3D conductive wrapping of graphene/MnO<sub>2</sub> nanostructured electrodes with CNTs or conducting polymer, we can optimize the electrochemical utilization of highly insulating MnO<sub>2</sub> materials and greatly enhance their supercapacitor performance. The rationally designed composite electrodes exhibit high specific capacitance, excellent rate capability, and exceptional cycling stability. Such a 3D conductive wrapping approach represents an effective and convenient technique to improve the specific capacitance and rate capability of oxide-based supercapacitors and can be applicable to a wide range of insulating energy storage electrode materials such as sulfur, LiMnPO<sub>4</sub>, and silicon in lithium-ion batteries. For example, conductive polymer can be used for wrapping sulfur cathode materials to enhance electrode conductivity and contain polysulfide intermediates, therefore minimizing polysulfide dissolution and improving the performance of Li–S batteries.

## ■ ASSOCIATED CONTENT

**S Supporting Information.** Details on materials and methods. This material is available free of charge via the Internet at <http://pubs.acs.org>.

## AUTHOR INFORMATION

### Corresponding Author

\*E-mail: yicui@stanford.edu; zbao@stanford.edu.

## ACKNOWLEDGMENT

Y.C. and Z.B. acknowledge the funding support from the Precourt Institute for Energy at Stanford University. Y.C. also acknowledges the funding support from the King Abdullah University of Science and Technology (KAUST) Investigator Award (No. KUS-11-001-12).

## REFERENCES

- (1) Burke, A. *J. Power Sources* **2000**, *91*, 37–50.
- (2) Conway, B. E. *Electrochemical Supercapacitors: Scientific Fundamentals and Technological Applications*; Kluwer Academic/Plenum: New York, 1999.
- (3) Burke, A. *Electrochim. Acta* **2007**, *53*, 1083–1091.
- (4) Miller, J. R.; Simon, P. *Science* **2008**, *321*, 651–652.
- (5) Simon, P.; Gogotsi, Y. *Nat. Mater.* **2008**, *7*, 845–854.
- (6) Cottineau, T.; Toupin, M.; Delahaye, T.; Brousse, T.; Bélanger, D. *Appl. Phys. A: Mater. Sci. Process.* **2006**, *82*, 599–606.
- (7) Toupin, M.; Brousse, T.; Belanger, D. *Chem. Mater.* **2004**, *16*, 3184–3190.
- (8) Wang, D.-W.; Li, F.; Cheng, H.-M. *J. Power Sources* **2008**, *185*, 1563–1568.
- (9) Bélanger, D.; Brousse, T.; Long, J. W. *Electrochem. Soc. Interfaces* **2008**, *17*, 49–52.
- (10) Lang, X.; Hirata, A.; Fujita, T.; Chen, M. *Nat. Nanotechnol.* **2011**, *6*, 232–236.
- (11) Ma, S.-B.; Nam, K.-W.; Yoon, W.-S.; Yang, X.-Q.; Ahn, K.-Y.; Oh, K.-H.; Kim, K.-B. *J. Power Sources* **2008**, *178*, 483–489.
- (12) Sivakkumar, S. R.; Ko, J. M.; Kim, D. Y.; Kim, B. C.; Wallace, G. G. *Electrochim. Acta* **2007**, *52*, 7377–7385.
- (13) Lee, S. W.; Kim, J.; Chen, S.; Hammond, P. T.; Shao-Horn, Y. *ACS Nano* **2010**, *4*, 3889–3896.
- (14) Hu, L.; Pasta, M.; Mantia, F. L.; Cui, L.; Jeong, S.; Deshazer, H. D.; Choi, J. W.; Han, S. M.; Cui, Y. *Nano Lett.* **2010**, *10*, 708–714.
- (15) Yan, J.; Fan, Z.; Wei, T.; Qian, W.; Zhang, M.; Wei, F. *Carbon* **2010**, *48*, 3825–3833.
- (16) Yu, G.; Hu, L.; Vosgueritchian, M.; Wang, H.; Xie, X.; McDonough, J. R.; Cui, X.; Cui, Y.; Bao, Z. *Nano Lett.* **2011**, *11*, 2905–2911.
- (17) Liu, R.; Lee, S. B. *J. Am. Chem. Soc.* **2008**, *130*, 2942–2943.
- (18) Chen, L.; Sun, L.-J.; Luan, F.; Liang, Y.; Li, Y.; Liu, X.-X. *J. Power Sources* **2010**, *195*, 3742–3747.
- (19) Hou, Y.; Cheng, Y.; Hobson, T.; Liu, J. *Nano Lett.* **2010**, *10*, 2727–2733.
- (20) Izadi-Najafabadi, A.; Yasuda, S.; Kobashi, K.; Yamada, T.; Futaba, D. N.; Hatori, H.; Yumura, M.; Iijima, S.; Hata, K. *Adv. Mater.* **2010**, *22*, E235–E241.
- (21) Wu, Z.-S.; Ren, W.; Wang, D.-W.; Li, F.; Liu, B.; Cheng, H.-M. *ACS Nano* **2010**, *4*, 5835–5842.
- (22) Chen, S.; Zhu, J.; Wu, X.; Han, Q.; Wang, X. *ACS Nano* **2010**, *4*, 2822–2830.
- (23) Naoi, K.; Simon, P. *Electrochem. Soc. Interface* **2008**, *17*, 34–37.